

OPEN ACCESS

EDITED BY

Tzu-Wei Fang,
Space Weather Prediction Center
(NOAA), United States

REVIEWED BY

Tibor Durgonics,
University of Colorado Boulder, United
States
Kshitija Deshpande,
Embry–Riddle Aeronautical University,
United States

*CORRESPONDENCE

Sebastijan Mrak,
✉ sebastijan.mrak@colorado.edu

SPECIALTY SECTION

This article was submitted to Space
Physics, a section of the journal
Frontiers in Astronomy and Space
Sciences

RECEIVED 06 November 2022

ACCEPTED 06 February 2023

PUBLISHED 16 February 2023

CITATION

Mrak S, Coster AJ, Groves K and Nikoukar
R (2023), Ground-based infrastructure
for monitoring and characterizing
intermediate-scale ionospheric
irregularities at mid-latitudes.
Front. Astron. Space Sci. 10:1091340.
doi: 10.3389/fspas.2023.1091340

COPYRIGHT

© 2023 Mrak, Coster, Groves and
Nikoukar. This is an open-access article
distributed under the terms of the
[Creative Commons Attribution License
\(CC BY\)](https://creativecommons.org/licenses/by/4.0/). The use, distribution or
reproduction in other forums is
permitted, provided the original author(s)
and the copyright owner(s) are credited
and that the original publication in this
journal is cited, in accordance with
accepted academic practice. No use,
distribution or reproduction is permitted
which does not comply with these terms.

Ground-based infrastructure for monitoring and characterizing intermediate-scale ionospheric irregularities at mid-latitudes

Sebastijan Mrak^{1*}, Anthea J. Coster², Keith Groves³ and Romina Nikoukar⁴

¹Space Weather Technology, Research, and Education Center, University of Colorado Boulder, Boulder, CO, United States, ²Haystack Observatory Massachusetts Institute of Technology, Westford, MA, United States, ³Institute for Scientific Research, Boston College, Boston, MA, United States, ⁴Applied Physics Laboratory, Johns Hopkins University, Laurel, MD, United States

We discuss potential science investigations at mid-latitudes enabled by a modern, space-weather-grade, ground-based Radio-Frequency network of scintillation receivers which encompasses Global Navigation Satellite Systems and Beacon receivers, along with coherent radars, and leveraging radio astronomy infrastructure for space weather application. The primary scientific research addresses the controlling space weather drivers for the structuring of mid-latitude ionospheric plasma at intermediate scales (10s of meters—10s of kilometers), their relationship with larger density structures, and their impacts on the trans-ionospheric radio links. These irregularities scintillate the signals impairing the radio link integrity and the underpinning services. The suggested science investigations are currently unable to be fully accomplished because of missing high-fidelity and long-term observations at satisfactory spatial coverage. We discuss the physics responsible for the radio wave disturbances and their impacts, review the current state of knowledge based on available observations, and outline a plan for developing the necessary infrastructure by leveraging existing ground-based distributed observatories that will enable novel scientific investigations and will be synergistic with other geoscience divisions such as seismology, geology, and meteorology.

KEYWORDS

ionospheric irregularities, scintillation, GNSS, plasma turbulence, space weather

1 Introduction

Ionospheric density irregularities are the primary space weather source of RF interference on the transionospheric radio links impairing the RF signals at frequencies ≤ 2 GHz including GNSS positioning and navigation service and high-frequency (HF) radars and communications. These ionospheric irregularities span over several orders of magnitude in spatial scales (meters to 100s of km) making them “visible” in HF radars such as the Super Dual Auroral Radar Network (SuperDARN) (Ribeiro et al., 2012; Nishimura et al., 2021; Nishimura et al., 2022), HAM radio links (Frissell et al., 2022), ionosondes (Zabotin and Wright, 2001), VHF coherent radars (Hysell and Larsen, 2021), and GNSS links (Mrak et al., 2018; Mrak et al., 2020; Mrak et al., 2021b). These ionospheric irregularities impact the HF systems by increasing uncertainties in ionospheric reflection

point and propagation direction, and by imposing rapid fluctuations in signal intensity and phase. GNSS services are impaired by these rapid signal fluctuations causing GNSS scintillation, cycle slips, and loss of lock. While climatology and occurrence of GNSS scintillation occurrence have been relatively well understood for low- and high-latitudes (e.g., Alfonsi et al., 2011; Jiao and Morton, 2015; de Oliveira Moraes et al., 2017), we do not yet have a clear understanding of GNSS scintillation-producing irregularities at mid-latitudes. It is known that mid-latitude irregularities are, on average, weak (Aarons, 1982; Kintner et al., 2007) and cause little to no impacts on ground-based GNSS services. However, weak irregularities impact GNSS Radio Occultation (RO) frequently at mid-latitudes (Watson and Pedatella, 2018) owing to highly oblique propagation geometry. The advent of new GNSS RO constellations in high inclination orbits now encounter these irregularities every orbit. Furthermore, recent observations using ground-based GNSS receivers revealed that GNSS scintillation were occasionally observed at mid-latitudes during moderate geomagnetic storms (e.g., Mrak et al., 2021a; Rodrigues et al., 2021, and discussed below). Because the world's population primarily lives in the mid-latitudes, it is imperative to better understand the controlling drivers causing mid-latitude plasma structuring, its climatology, controlling, and geophysical drivers.

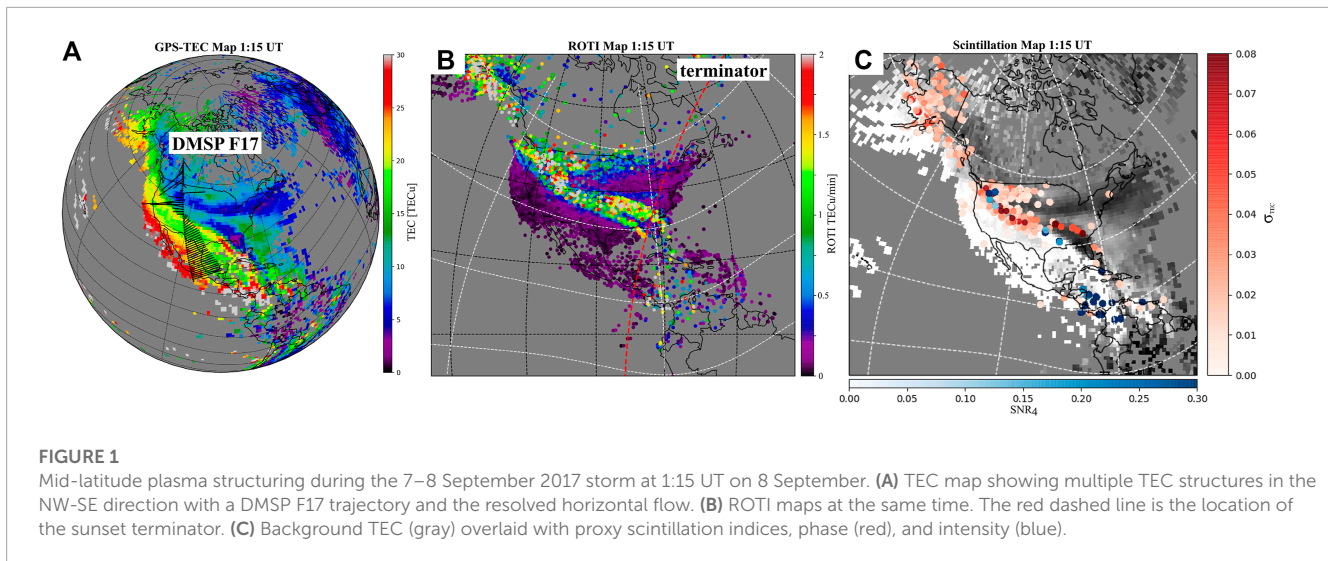
Ionospheric density irregularities refract radio waves due to changing index of refraction n , whose magnitude changes with the RF frequency f and plasma density n_e . If the geometry of the radio link (distance between the irregularities and the receiver R), frequency f , and the irregularities' spatial scale (projection in the perpendicular direction (x, y) relative to the radio waves propagation z) is $\rho = \sqrt{x^2 + y^2}$ are in fortuitous agreement, then refracted radio waves interfere while propagating to the receiver—causing the diffraction. In the phase screen approximation (Booker et al., 1950; Rino, 1979), the maximum diffraction is caused by irregularities with spatial scales around $\rho = \rho_F = \sqrt{2\lambda R}$, where ρ_F is the Fresnel scale, λ is the RF wavelength ($\lambda = c_0/f$, where c_0 is the speed of light) assuming R to be much smaller than the distance from the transmitter to the irregularities. The diffraction is a high-pass filtering operation between the input radio wavefront and the 2-D irregularity field $\delta N_e(x, y)$. Therefore, only the portion of the irregularities near and smaller than the Fresnel scale contribute to the diffraction, but the total contribution is highly weighted towards ρ_F because of the exponential decrease in the density perturbation magnitude (δN_e) with decreasing scales. The strength of the diffraction is proportional to the δN_e , which controls the perturbations in the index of refraction that scales with $1/f^2$. Therefore, lower frequencies are affected more significantly because the same δN_e causes a bigger perturbation in the index of refraction. In aggregate, the impacts of ionospheric irregularities on the RF systems depend on the magnitude of the irregularities themselves, their spatial scales compared to the RF frequency, and the distance between the irregularities and RF receivers on the ground.

Mid-latitudes are constantly perturbed by internal and external forcing causing Medium Scale Traveling Ionospheric Disturbances (MSTIDs). The majority of these medium-scale disturbances are manifestations of gravity waves (Hernández-Pajares et al., 2006). These coherent perturbations have an impact on aided single-frequency (real-time kinematic) GNSS positioning (Timoté et al.,

2020) despite that their magnitude is only a ~ 0.1 TECu (1 TECu = 10^{16} electrons per m^2), which is only a few % of the background TEC. Mid-latitude MSTIDs during geomagnetically disturbed times can reach amplitudes of >10 TECu as depicted in Figure 1A. These perturbations were associated with large ion drifts as indicated by the black vectors along a satellite trajectory. These MSTID-like structures were co-located with ionospheric irregularities measured by the Rate of TEC change Index (ROTI) in Figure 1B, and with GNSS scintillation-producing irregularities depicted in Figure 1B (e.g., Mrak et al., 2020). Additionally, there was a presence of elevated SuperDARN backscatter co-located with the structures (Nishimura et al., 2021). These multi-scale irregularities caused a significant increase in GNSS positioning errors where 50% of mid-latitude stations exhibited 1–3 m errors (Yang et al., 2020) (the normal 3D error is ~ 10 cm) using Precise Point Positioning (PPP) methodology. Additionally, this storm caused reduced availability of GNSS-assisted systems such as the European Geostationary Navigation Overlay Service (EGNOS) (Berdermann et al., 2018). The underlying conditions causing these medium-scale perturbations and the destabilizing mechanisms causing (turbulent) decay are not yet understood. The referred case study used a single, Global Positioning System (GPS) constellation in a post-processing set-up. The actual position error depends on several technical aspects such as the number of total visible satellites (i.e., the number of constellations tracked), and processing parameters where the most critical aspect is cycle slip mitigation. Thus, the errors depend on the PPP time resolution and number of satellites in view (Bahadur and Nohutcu, 2020).

The first reported GNSS scintillation measurements at mid-latitudes were observed from upstate New York, during a moderate storm on the 24–25 September 2001 (Ledvina et al., 2002). A recent survey for GNSS scintillation events found nine storms with average peak Dst = -131 nT, and $K_p = 7^-$, that caused observable scintillations at mid-latitudes (Mrak et al., 2021a). The majority of events resembled extreme poleward expansion of Equatorial Plasma Bubbles (EPBs). EPBs are often recognized as the most severe space weather threat to the reliability of the GNSS services, thereby these findings are striking both in terms of space weather impacts and the underlying physical mechanisms responsible for the EPB expansion to mid-latitudes. A case study using co-located GNSS scintillation and airglow observations showed what seems to be EPB-like events causing moderate to strong GNSS scintillation reaching as far as Texas (Rodrigues et al., 2021). These observations were made using proxy observations for the conventional scintillation indices or a single Ionospheric Scintillation Monitoring Receiver (ISMR), making the observations impossible to estimate the statistical properties of the underlying intermediate-scale irregularities.

Currently, we do not have the capabilities to readily observe intermediate-scale ionospheric irregularities (10s of meters to 10s of kilometers) at mid-latitudes (we define mid-latitudes as the region between $30 \leq |\text{MLAT}| \leq 60$). Here we focus on the American longitude sector $60^\circ\text{W} \leq \text{LON} \leq 130^\circ\text{W}$, but the measurements are missing globally at mid-latitudes. GNSS scintillation observations are normally taken by ISMRs providing high-fidelity phase and amplitude data at 50–100 Hz resolution. Alternatively, GNSS scintillation data can be taken from low-earth orbiting satellites with GNSS-RO probing the ionosphere at



highly oblique angles. High-fidelity and open-source GNSS-RO missions were Constellation Observing System for Meteorology Ionosphere and Climate (COSMIC) and COSMIC-2, but with only sporadic coverage over mid-latitudes. Mid-latitude Ionospheric irregularities were ubiquitous in the COSMIC data (Watson and Pedatella, 2018). Note the GNSS-RO signals scintillate due to larger irregularities ($\rho \approx$ kilometers) because the responsible irregularities are considerably further away (i.e., larger R) from the receiver compared to ground-based receivers, causing larger Fresnel scale ρ_F . The science avenues enabled by the GNSS-RO are promising considering auxiliary commercial GNSS-RO data provided through the NASA Commercial SmallSat Data Acquisition (CSDA) program in addition to the COSMIC-2. On the contrary, ground-based facilities providing GNSS and RF space weather data at lower frequencies need substantial investments to bridge the data gap. We discuss how the deployment of space weather-grade infrastructure including high-fidelity and low-cost ISMRs (Rodrigues and Moraes, 2019), Very High Frequency (VHF)/Ultra High Frequency (UHF) beacon receivers (e.g., Bernhardt et al., 2006), and coherent scatter radars (Hysell and Burcham, 2000; Huyghebaert et al., 2019), can bridge this observational gap.

2 Discussion

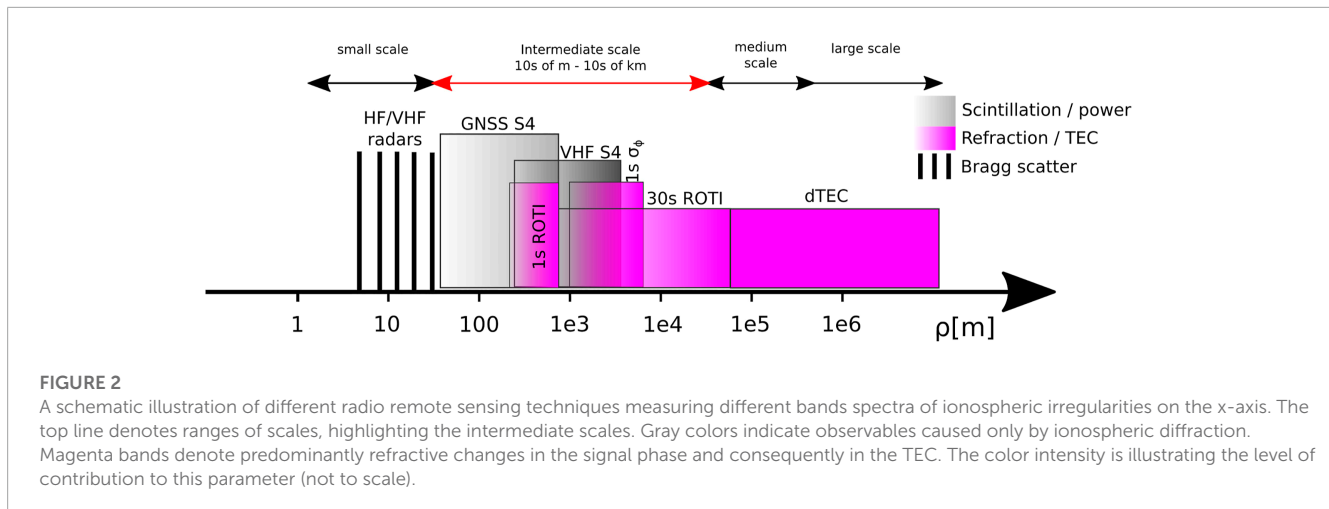
We discuss observing techniques needed to observe intermediate-scale irregularities and propose a deployment strategy with operational relevance.

2.1 Observing intermediate-scale irregularities

Ionospheric RF monitoring platforms measure the signal's power and phase at multiple frequencies and output several observing quantities (derived from measurements): scintillation

indices, TEC from dual-frequency measurements, and Rate of TEC change Index (ROTI). In addition, the coherent radars measure the Bragg backscatter from irregularities at $\rho = \lambda/2$; spanning from $\rho = 3$ m for the ICEBEAR radar (Huyghebaert et al., 2019) to $\rho = 15$ m to Super Dual Auroral Radar Network (SuperDARN) (Ribeiro et al., 2012) providing high-fidelity and continuous observations of small-scale irregularities in at several longitudinal sectors of mid-latitudes in the northern hemisphere. The use of these observations could be thought of as a filter bank with varying bandwidth for observing intermediate scale irregularities as illustrated in Figure 2.

Radio scintillation is normally measured using scintillation indices $S_4^2 = (\langle P^2 \rangle - \langle P \rangle^2) / \langle P \rangle^2$ indicating fluctuations in signal's power P , and $\sigma_\phi^2 = \langle \phi^2 \rangle - \langle \phi \rangle^2$ indicating fluctuations in signal's phase ϕ . The brackets denote temporal averaging over 1 min. Phase is conventionally high-pass filtered at a cutoff frequency $f_c = 0.1$ Hz (Mrak et al., 2018, and the references therein) to isolate the high-frequency fluctuations. Diffraction is caused by irregularities with scale sized below the Fresnel scale, $\rho \leq 500$ m and $\rho \leq 1.5$ km for GNSS frequencies (1.1–1.6 GHz) and VHF/UHF beacon frequencies (100–500 MHz). Diffraction is depicted as gray band-pass filters in Figure 2, where the lower boundary is fuzzily denoted by light shading because the contributions from smaller scales decrease exponentially. Phase scintillation index σ_ϕ is sensitive to perturbations with periods below 10 s (high pass filter cutoff) including the diffraction, translating to irregularity scales below 5 km. The lower boundary is determined by the receiver sampling which is 1 km for receivers with 1-s data resolution (i.e., 2-s Nyquist period) ROTI was proposed as a measure of ionospheric irregularities (Pi et al., 1997) and is readily used today. ROTI measures a sum of all changes in the TEC between two consecutive samples δt apart. For 30-s resolution data, ROTI measures TEC perturbations at scales below ~ 20 km, whereas the 1-s resolution data measures TEC perturbations below 500 m, assuming the same drift velocity. Phase observations are not Fresnel filtered, whereas intensity measures



are. Contributions from refraction are noted as magenta shading in **Figure 2**, with lighter hue intensity at smaller scales indicating their smaller relative contribution. Lastly, the coherent radars measure irregularities at a very narrow bandwidth corresponding to the Bragg criteria, sampling the irregularity spectrum at a delta function. All the assumptions converting the temporal scales t/f (measured) to spatial scales ρ/k (inferred) are obtained by assuming a linear relationship f [Hz] = k [m^{-1}] v [m/s], where $v = 500$ m/s is the irregularity drift velocity projection in a direction perpendicular to the propagation (Carrano et al., 2019; Mrak et al., 2021a). Lastly, maps of differential TEC using detrended from 30-s resolution data provide auxiliary measurements of medium (50–1000 km) and large-scale (>1000 km) TIDs. Combining all the observing modalities together, one can observe a whole spectrum of ionospheric irregularities from small scales to large scales, including the intermediate-scale irregularities that are responsible for scintillation. Currently, we can readily observe irregularities at medium- and large scales from dense 30-s GNSS networks, and small scales using the SuperDARN radars. The gap between these regions—intermediate-scale irregularities—is only partially covered with geodetic 1-s resolution GNSS receivers with limited observing capabilities (cf. Mrak et al., 2020).

Measuring all the different parameters needed to cover the intermediate-scale irregularity spectra is not strictly necessary, if relationships among S_4 , σ_ϕ , and ROTI can be exploited. Carrano et al. (2019) presented an analytical derivation of the relationship between the S_4 and ROTI, assuming the weak scatter theory, showing that they are related by the irregularity drift velocity v . They successfully validated this approach using 1-s ROTI and v derived from two closely spaced antennas using a separate geostationary link. Exploiting 1-s ROTI is promising at mid-latitudes because hundreds of geodetic receivers could be leveraged to estimate scintillation *via* S_4 (Mrak et al., 2020). However, there are several caveats tied to this relationship: (1) v has to be estimated independently for each receiver station. At low-latitudes, v varies between ~50–200 m/s, whereas at mid-latitudes it can exceed 1 km/s (Foster and Rich, 1998; Mishin and Blaunstein, 2008; song Huang et al., 2007; Nishimura et al., 2021) making this

endeavor difficult. (2) the derivation assumes the known outer and inner scale of the irregularity spectrum and known irregularity axial ratio. These assumptions can be fixed at low-latitudes with high confidence because they were studied in detail there and they do not vary much. However, we do not know them well at mid-latitudes. Carrano et al. (2016) introduced an alternative approach for estimating v from σ_ϕ and S_4 . This approach relies on the same assumptions as the S_4 -ROTI relationship, and it requires S_4 and σ_ϕ —which can be only acquired with an ISMR anyway. Additionally, it has been demonstrated that the definition of the σ_ϕ is not valid for larger velocities v expected at mid-latitudes (Spogli et al., 2022). A more reliable alternative for estimating v is the utilization of GNSS receiver network by performing cross-correlation analysis in a space-time domain as demonstrated on several regional networks (Watson et al., 2011; Wang and Morton, 2015; Nishimura et al., 2022), with the only assumption being the separation between the ionospheric piercing points being shorter than the decorrelation length of irregularities.

The filter bank measurement approach using scintillation could be augmented to higher scales with more sensitive RF infrastructure at VHF and UHF frequencies using beacon receivers (Bernhardt et al., 2006; Carrano and Groves, 2006) and bright cosmic radio sources at frequencies between 10–90 MHz. These can be accomplished by leveraging the radio astronomy radio telescopes such as Low-Frequency Array (LOFAR) (Fallows et al., 2020), Long Wavelength Array (LWA) (Breen et al., 2008) and a simplified interferometer using two LWA antennas—Deployable Low-band Ionosphere and Transient Experiment (DLITE) (Helmboldt and Zobotin, 2022). LOFAR has in particular great potential for measuring ionospheric scintillation because it consists of many receiver stations covering a large swath of the European longitude sector freely available data though the long term storage archive (<https://lta.lofar.eu/>). Currently, only the COSMIC-2 constellation broadcasts continuous UHF beacon but it is under utilized for scientific exploration, and has a poor coverage over the mid-latitudes. The addition of VHF/UHF monitoring ionospheric scintillation increases direct measurements of scintillation-producing intermediate scale irregularities to >3 km using

astronomical radio sources (i.e., [Fallows et al., 2020](#)), or new satellite constellations with VHF/UHF beacon payloads with beacon receiver segments (e.g., ?).

In aggregate, scintillation-producing intermediate-scale irregularities can be directly measured and characterized by ISMRs. Covering large, continental-scale, areas with ISMRs would be an expensive and logistically tedious effort. Alternative routes using inexpensive scintillation receivers ([Rodrigues and Moraes, 2019](#)), and leveraging existing geodetic receivers with 1-s data ([Mrak et al., 2020](#)) using S_4 -ROTI relationship ([Carrano et al., 2019](#)) can augment the high-fidelity measurements adequately if the sensor network(s) are deployed in an intelligent topology. Years of observations would be likely needed to derive empirical relationships between S_4 , σ_ϕ , ROTI, and ν at mid-latitudes under varying geophysical conditions.

2.2 Enabling scientific investigations

A distributed network of RF observatories for space weather, covering the entire continental United States and capable of making high-rate scintillation measurements, would enable observations of intermediate-scale ionospheric irregularities, their spatiotemporal evolution, and occurrence, and support analysis of their impacts on the GNSS services. By combining these new observations with the TEC and detrended TEC maps, from data already available from 30-s resolution receivers, these irregularities will be put into a context of larger-medium and large-scale-density structures and gradients. The new observations will enable scientific investigations related to but not limited to density irregularities associated with mid-latitude trough and related phenomena (subauroral polarization streams, Strong Thermal Emission Velocity Enhancement STEVE), storm enhanced density, mid-latitude spread F, EPBs penetrating to mid-latitudes, decaying MSTIDs. In order to understand the underlying physical mechanisms producing the intermediate-scale irregularities, employing suitable physics-based models reproducing ionospheric plasma instabilities is necessary. The modeling support is a separate problem that we cannot address. Spatially distributed and high-fidelity observations of intermediate-scale irregularities covering a whole continent will enable the quantification of:

- What is the occurrence of mid-latitude intermediate-scale irregularities during quiet and disturbed conditions?
- What are the controlling space weather parameters (solar wind, interplanetary magnetic field, penetration electric field, auroral activity), local time, and longitude dependence?
- Where do these irregularities reside with respect to the larger density structures and gradients?
- What are the physical mechanisms producing the intermediate-scale irregularities at mid-latitudes?
- Are these irregularities coupled to high- or low-latitude dynamics or are they created *in situ* at mid-latitudes?

2.3 Deployment strategy and data utilization

The backbone infrastructure supporting distributed ground-based observatories already exists in the US and Europe: this includes the physical sites where instrumentation is deployed and running, with established data acquisition, storage, and user access. We urge the agencies to leverage the available existing infrastructure for the space-weather-qualified instrumentation and data products described in this report. National Science Foundation (NSF) and the National Aeronautics and Space Administration (NASA) have been funding large networks of ground-based instrumentation for decades such as the UNAVCO's GAGE facility consisting of a network of GNSS receivers providing 1-s and 30-s data. National Geodetic Survey, part of the National Oceanic and Atmospheric Agency (NOAA) operates a Continuously Operating Receiver Stations (CORS) Network (NCN) providing GNSS data at 30-s resolution. NCN aggregates data from many different providers and distributes the data from a single end-point interface. Additional investments to upgrade the available infrastructure and accommodate the deployment of additional ISMRs and beacon receivers would, in addition to enabling space weather research, increase the quality of GNSS data for a wide range of applications making the investment highly synergistic with the other fields such as seismology, geology, and meteorology.

The standardized data outputs with long-term storage should consist of: 1) RINEX files at 1-s and 30-s resolution used to compute TEC and ROTI. 2) The new network(s) with ISMRs should provide additional files with derived scintillation indices S_4 and σ_ϕ , and the decorrelation times derived from 50 to 100 Hz measurements. 3) The new networks should store raw 50–100 Hz power and phase (or I and Q) measurements for retrospective analyses, providing these data upon request using online interfaces.

Auxiliary VHF/UHF beacon receivers and LWA receivers can be deployed at hosting institutions because the operations and hardware are more involved compared to the plug-and-play nature of GNSS receiver technology. The deployment could involve higher education institutions, radio enthusiasts such as HAM radio operators, and observatories.

2.4 Relevance to research-to-operations

Space Weather Prediction Center (SWPC) currently observes ionospheric irregularities using ROTI derived from 30-s resolution data. A machine learning algorithm is then applied to these ROTI maps to identify advisory polygons—regions with potential impact on the GNSS users. The new distributed observatory measuring intermediate-scale irregularities in concert with leveraging the 1-s ROTI maps as a proxy measure of scintillation ([Carrano et al., 2019](#)) can provide SWPC with upgraded advisory polygons using the actual scintillation observation. The addition of scintillation observations from VHF receivers could potentially yield a new operational product advising HF communication disruptions.

Data availability statement

The original contributions presented in the study are included in the article/supplementary material, further inquiries can be directed to the corresponding author.

Author contributions

SM conceptualized this study and wrote the first draft of the manuscript. AC, KG, and RN contributed text to parts of the manuscript. All authors contributed to the manuscript revision, read, and approved the submitted version.

Funding

This study was partially funded by NASA grant 80NSSC21K1321 to the University of Colorado Boulder. This work was catalyzed by the NASA Living With a Star Institute on TEC and Scintillation. This research was supported by the International

Space Science Institute (ISSI) in Bern and Beijing, through ISSI International Team project #511 (Multi-Scale Magnetosphere-Ionosphere-Thermosphere Interaction).

Conflict of interest

The authors declare that the research was conducted in the absence of any commercial or financial relationships that could be construed as a potential conflict of interest.

Publisher's note

All claims expressed in this article are solely those of the authors and do not necessarily represent those of their affiliated organizations, or those of the publisher, the editors and the reviewers. Any product that may be evaluated in this article, or claim that may be made by its manufacturer, is not guaranteed or endorsed by the publisher.

References

- Aarons, J. (1982). Global morphology of ionospheric scintillations. *Proc. IEEE* 70, 360–378. doi:10.1109/PROC.1982.12314
- Alfonsi, L., Spogli, L., Franceschi, G. D., Romano, V., Aquino, M., Dodson, A., et al. (2011). Bipolar climatology of gps ionospheric scintillation at solar minimum. *Radio Sci.* 46. doi:10.1029/2010rs004571
- Bahadur, B., and Nohutcu, M. (2020). Impact of observation sampling rate on multi-gnss static ppp performance. *Surv. Rev.* 0, 206–215. doi:10.1080/00396265.2019.1711346
- Berdermann, J., Kriegel, M., Banyś, D., Heymann, F., Hoque, M. M., Wilken, V., et al. (2018). Ionospheric response to the x9.3 flare on 6 september 2017 and its implication for navigation services over Europe. *Space weather*. 16, 1604–1615. doi:10.1029/2018SW001933
- Bernhardt, P., Siefring, C., and Wilkens, M. (2006). “Multi-frequency satellite beacons and receivers for ionospheric irregularity imaging,” in 2006 10th IET International Conference on Ionospheric Radio Systems and Techniques (IRST 2006) (IEEE), 198–201. doi:10.1049/cp:20060266
- Booker, H. G., Ratcliffe, J. A., and Shinn, D. H. (1950). Diffraction from an irregular screen with applications to ionospheric problems. *Philosophical Trans. R. Soc. Lond. Ser. A, Math. Phys. Sci.* 242, 579–607. doi:10.1098/rsta.1950.0011
- Breen, A. R., Fallows, R. A., Bisi, M. M., Jones, R. A., Jackson, B. V., Kojima, M., et al. (2008). The solar eruption of 2005 may 13 and its effects: Long-baseline interplanetary scintillation observations of the earth-directed coronal mass ejection. *Astrophysical J.* 683, L79–L82. doi:10.1086/591520
- Carrano, C. S., Groves, K. M., Rino, C. L., and Doherty, P. H. (2016). A technique for inferring zonal irregularity drift from single-station gnss measurements of intensity (s_4) and phase (σ_ϕ) scintillations. *Radio Sci.* 51, 1263–1277. doi:10.1002/2015RS005864
- Carrano, C. S., Groves, K. M., and Rino, C. L. (2019). On the relationship between the rate of change of total electron content index (ROTI), irregularity strength ($C^{\circ}KL$), and the scintillation index ($S^{\circ}4$). *J. Geophys. Res. Space Phys.* 124, 2099–2112. doi:10.1029/2018JA026353
- Carrano, C. S., and Groves, K. M. (2006). The gps segment of the afrl-scinda global network and the challenges of real-time tec estimation in the equatorial ionosphere. *Proc. Inst. Navigation, Natl. Tech. Meet.* 2, 1036–1047.
- de Oliveira Moraes, A., Costa, E., Abdu, M. A., Rodrigues, F. S., de Paula, E. R., Oliveira, K., et al. (2017). The variability of low-latitude ionospheric amplitude and phase scintillation detected by a triple-frequency gps receiver. *Radio Sci.* 52, 439–460. doi:10.1002/2016RS006165
- Fallows, R. A., Forte, B., Astin, I., Allbrook, T., Arnold, A., Wood, A., et al. (2020). A lofar observation of ionospheric scintillation from two simultaneous travelling ionospheric disturbances. *J. Space Weather Space Clim.* 10, 10. doi:10.1051/swsc/2020010
- Foster, J. C., and Rich, F. J. (1998). Prompt midlatitude electric field effects during severe geomagnetic storms. *J. Geophys. Res. Space Phys.* 103, 26367–26372. doi:10.1029/97JA03057
- Frissell, N. A., Kaeppeler, S. R., Sanchez, D. F., Perry, G. W., Engelke, W. D., Erickson, P. J., et al. (2022). First observations of large scale traveling ionospheric disturbances using automated amateur radio receiving networks. *Geophys. Res. Lett.* 49. doi:10.1029/2022GL097879
- Helmboldt, J. F., and Zabotin, N. (2022). An observed trend between mid-latitudes km-scale irregularities and medium-scale traveling ionospheric disturbances. *Radio Sci.* 57, e2021RS007396. doi:10.1029/2021RS007396
- Hernández-Pajares, M., Juan, J. M., and Sanz, J. (2006). Medium-scale traveling ionospheric disturbances affecting gps measurements: Spatial and temporal analysis. *J. Geophys. Res.* 111, A07S11. doi:10.1029/2005JA011474
- Huyghebaert, D., Hussey, G., Vierinen, J., McWilliams, K., and St-Maurice, J. (2019). Icebear: An all-digital bistatic coded continuous-wave radar for studies of the e region of the ionosphere. *Radio Sci.* 54, 349–364. doi:10.1029/2018RS006747
- Hysell, D. L., and Burcham, J. D. (2000). The 30-mhz radar interferometer studies of midlatitude e region irregularities. *J. Geophys. Res. Space Phys.* 105, 12797–12812. doi:10.1029/1999JA000411
- Hysell, D. L., and Larsen, M. F. (2021). Vhf imaging radar observations and theory of banded midlatitude sporadic e ionization layers. *J. Geophys. Res. Space Phys.* 126. doi:10.1029/2021JA029257
- Jiao, Y., and Morton, Y. T. (2015). Comparison of the effect of high-latitude and equatorial ionospheric scintillation on gps signals during the maximum of solar cycle 24. *Radio Sci.* 50, 886–903. doi:10.1002/2015RS005719
- Kintner, P. M., Ledvina, B. M., and de Paula, E. R. (2007). Gps and ionospheric scintillations. *Space weather*. 5. doi:10.1029/2006SW000260
- Ledvina, B. M., Makela, J. J., and Kintner, P. M. (2002). First observations of intense gps l1 amplitude scintillations at midlatitude. *Geophys. Res. Lett.* 29, 4-1–4-4. doi:10.1029/2002GL014770
- Mishin, E., and Blaunstein, N. (2008). “Irregularities within subauroral polarization stream-related troughs and gps radio interference at midlatitudes,” in *Midlatitude Ionospheric Dynamics and Disturbances*. Editors P. M. Kintner, A. J. Coster, T. Fuller-Rowell, A. J. Mannucci, M. Mendillo, and R. Heelis, doi:10.1029/181GM26
- Mrak, S., Semeter, J., Hirsch, M., Starr, G., Hampton, D., Varney, R. H., et al. (2018). Field-aligned gps scintillation: Multisensor data fusion. *J. Geophys. Res. Space Phys.* 123, 974–992. doi:10.1002/2017JA024557

- Mrak, S., Semeter, J., Nishimura, T., Coster, A. J., and Groves, K. (2021a). "Space weather at mid-latitudes: Leveraging geodetic gps receivers for ionospheric scintillation science," in 34th International Technical Meeting of the Satellite Division of The Institute of Navigation, 3910–3919. doi:10.33012/2021.18130
- Mrak, S., Semeter, J., Nishimura, Y., and Coster, A. J. (2021b). Extreme low-latitude total electron content enhancement and global positioning system scintillation at dawn. *Space weather*. 19. doi:10.1029/2021SW002740
- Mrak, S., Semeter, J., Nishimura, Y., Rodrigues, F. S., Coster, A. J., and Groves, K. (2020). Leveraging geodetic gps receivers for ionospheric scintillation science. *Radio Sci.* 55, 1–17. doi:10.1029/2020RS007131
- Nishimura, Y., Goldstein, J., Martinis, C., Ma, Q., Li, W., Zhang, S. R., et al. (2022). Multi-scale density structures in the plasmaspheric plume during a geomagnetic storm. *J. Geophys. Res. Space Phys.* 127. doi:10.1029/2021JA030230
- Nishimura, Y., Mrak, S., Semeter, J. L., Coster, A. J., Jayachandran, P. T., Groves, K. M., et al. (2021). Evolution of mid-latitude density irregularities and scintillation in North America during the 7–8 september 2017 storm. *J. Geophys. Res. Space Phys.* 126, 2–31. doi:10.1029/2021JA029192
- Pi, X., Mannucci, A. J., Lindqwister, U. J., and Ho, C. M. (1997). Monitoring of global ionospheric irregularities using the worldwide gps network. *Geophys. Res. Lett.* 24, 2283–2286. doi:10.1029/97GL02273
- Ribeiro, A. J., Ruohoniemi, J. M., Baker, J. B. H., Clausen, L. B. N., Greenwald, R. A., and Lester, M. (2012). A survey of plasma irregularities as seen by the midlatitude blackstone superdarn radar. *J. Geophys. Res. Space Phys.* 117. doi:10.1029/2011JA017207
- Rino, C. L. (1979). A power law phase screen model for ionospheric scintillation: 1. Weak scatter. *Radio Sci.* 14, 1135–1145. doi:10.1029/RS014i006p01135
- Rodrigues, F. S., and Moraes, A. O. (2019). Scintipi: A low-cost, easy-to-build gps ionospheric scintillation monitor for dasi studies of space weather, education, and citizen science initiatives. *Earth Space Sci.* 6, 1547–1560. doi:10.1029/2019EA000588
- Rodrigues, F. S., Socola, J. G., Moraes, A. O., Martinis, C., and Hickey, D. A. (2021). On the properties of and ionospheric conditions associated with a mid-latitude scintillation event observed over southern United States. *Space weather*. 19, 1–20. doi:10.1029/2021sw002744
- song Huang, C., Foster, J. C., and Sahai, Y. (2007). Significant depletions of the ionospheric plasma density at middle latitudes: A possible signature of equatorial spread f bubbles near the plasmapause. *J. Geophys. Res. Space Phys.* 112. doi:10.1029/2007JA012307
- Spogli, L., Ghobadi, H., Cicone, A., Alfonsi, L., Cesaroni, C., Linty, N., et al. (2022). Adaptive phase detrending for gnss scintillation detection: A case study over Antarctica. *IEEE Geoscience Remote Sens. Lett.* 19, 1–5. doi:10.1109/LGRS.2021.3067727
- Timoté, C. C., Juan, J. M., Sanz, J., González-Casado, G., Rovira-García, A., and Escudero, M. (2020). Impact of medium-scale traveling ionospheric disturbances on network real-time kinematic services: Catnet study case. *J. Space Weather Space Clim.* 10, 29. doi:10.1051/swsc/2020030
- Wang, J., and Morton, Y. T. (2015). High-latitude ionospheric irregularity drift velocity estimation using spaced gps receiver carrier phase time–frequency analysis. *IEEE Trans. Geoscience Remote Sens.* 53, 6099–6113. doi:10.1109/TGRS.2015.2432014
- Watson, C., Jayachandran, P. T., Spanswick, E., Donovan, E. F., and Danskin, D. W. (2011). Gps tec technique for observation of the evolution of substorm particle precipitation. *J. Geophys. Res. Space Phys.* 116. doi:10.1029/2010JA015732
- Watson, C., and Pedatella, N. M. (2018). Climatology and characteristics of medium-scale f region ionospheric plasma irregularities observed by cosmic radio occultation receivers. *J. Geophys. Res. Space Phys.* 123, 8610–8630. doi:10.1029/2018JA025696
- Yang, Z., Mrak, S., and Morton, Y. J. (2020). "Geomagnetic storm induced mid-latitude ionospheric plasma irregularities and their implications for gps positioning over North America: A case study," in 2020 IEEE/ION Position, Location and Navigation Symposium (PLANS) (IEEE), 234–238. doi:10.1109/PLANS46316
- Zabotin, N. A., and Wright, J. W. (2001). Ionospheric irregularity diagnostics from the phase structure functions of mf/hf radio echoes. *Radio Sci.* 36, 757–771. doi:10.1029/2000RS002512